Semi-numerical Calculations on 3-D Simulation of MHD Peristaltic Pseudoplastic-Nanofluid Flow with Dependent-Conductivity for Energy-Efficient Building Systems

M. G. IBRAHIM[1,*], IBRAHIM. M. GOMAA[2], SAMAR EL-SAYED AHMED[3]
[1]Basic and Applied Science Department,
International Academy for Engineering and Media Science,
11311,
EGYPT

[2]ElSewedy University of Technology,
Basic Science Department,
EGYPT

[3]Architecture Engineering Department,
International Academy for Engineering and Media Science,
11311,
EGYPT

Abstract: - This study investigates the magnetohydrodynamic (MHD) flow, heat, and mass transfer of a pseudoplastic (non-Newtonian) nanofluid within a mixed convection channel. The analysis focuses on the coupled effects of temperature-dependent activation energy and variable electrical conductivity, governed by the Wiedemann-Franz law. An adaptive multi-step differential transform method (AM-DTM) is employed to solve the governing non-linear equations. The solutions characterize the behavior of a tabbed bolus, the velocity maximum, and the spatial distributions of velocity, temperature, and nanoparticle concentration. Model validation is achieved through numerical comparison with nearest published results. Key findings indicate that elevated temperature- and concentration-dependent electrical conductivity enhances the potential energy of nanoparticles. This effect increases the temperature of the interior channel walls by 3–5 °C, a mechanism with potential applications for sustainable thermal management in building envelopes. Furthermore, modulation of thermophoresis and Brownian motion parameters provides effective control over the maximum flow velocity, thereby optimizing heat transfer rates. This optimization is directly relevant to improving thermal regulation in advanced solar cell systems. The absorption and transfer of solar thermal energy are critical in numerous industrial and architectural applications. The integration of nanofluids within building envelopes represents an innovative passive cooling strategy for sustainable architecture.

Key-Words: - Sustainable Architecture, Hybrid channel, Pseudoplastic nanofluid, adaptive multi-step differential transform method, Dependent - Electrical conductivity, Activation energy, WolframMathematica 14.2.

Received: July 13, 2025. Revised: October 25, 2025. Accepted: November 16, 2025. Published: December 31, 2025.

1 Introduction

In the early era, the precise operational benefits of peristaltic pumps have long attracted massive studies and modeling interest, pushed with the aid of using the want to apprehend the underlying fluid dynamics for important engineering applications. Primary implementations consist of the best thermal control of touchy electronics, wherein a peristaltic pump`s contamination-loose operation circulates ethanol via a closed silicone loop, subcooling it in a dry ice tub before extracting warmth from high-density cortical chips, [1]. In renewable power structures, those pumps are indispensable to energetic cooling circuits inside sun collectors, without delay improving thermal management and warmth switch coefficients to optimize photovoltaic performance post-power conversion, [2], [3] and [4]. Furthermore, their inherent reliability and unique volumetric management render them fundamental for high-performance thermal law in superior structures, substantially inside secondary cooling loops of nuclear reactors, [5].

More recently, the combination of non-Newtonian fluids, in particular pseudoplastic (shear-thinning) nanofluids, has extended the useful scope of those structures inside clever engineering and power-absorption processes. For instance, in solar power applications, the shear-thinning property wherein viscosity decreases beneathneath carried out stress allows engineered pseudoplastic nanofluid inks to facilitate homogeneous, strong layer deposition, making an allowance for high-precision, cost-effective printing of natural solar cells. In hybrid sun structures, such fluids also can function tunable dynamic optical filters, [6], [7]. Moreover, pseudoplastic conduct underpins superior clever window technology in power-green buildings, along with electrochromic or polymer-dispersed liquid crystal (PDLC) glass. Here, an electrically powered discipline induces shear, right away thinning the fluid to transition the window from an opaque to an obvious state. This allows real-time modulation of sun irradiance absorption, that may lessen HVAC power intake with the aid of using as a good deal as 30% [8], [9] and [10].

This technological development has stimulated targeted hydrodynamic studies. In the context of sun collectors, the influence of variable thermophysical properties on pseudoplastic nanofluid flow are studied, [11]. Concurrently, the results of chemical response at the magnetohydrodynamic (MHD) peristaltic shipping of a pseudoplastic nanofluid, incorporating Soret and Dufour cross-diffusion results discussed and reported [11] and [12]. These investigations shape a part of a broader studies initiative exploring non-Newtonian fluid dynamics throughout various engineering domains, [13].

The concept of a hybrid channel remains unexplored in fluid mechanics research. Existing research predominantly examines channels with symmetric or choppy uniform walls due to their relevance to physiological processes. For example, divergent-convergent choppy channel for Eyring fluid drift, noting that the pace of growth will grow with the non-uniform parameter is analyzed, [14]. On the Other study, a gyrotactic microorganisms in the blood drift internal and choppy channel, searching for a parabolic pace profile near the channel core is established, [15]. Furthermore, a symmetric channel with slip results on Powell fluid, finding that the trapped bolus duration decreases with positive fluid parameters is constructed, [16]. In the evaluation of the one's research, the winning artwork introduces a totally specific hybrid configuration, in which the pinnacle wall is uniform, and the lower wall is non-uniform, more studies of a symmetric channel can be found on [17], [18] .

The answers to such troubles are frequently derived from the use of linearization, perturbation techniques, or restrictive assumptions. In contrast, this has a take a observe employs the multi-degree differential redesign method (Ms-DTM) because it must address the surprisingly non-linear phrases inherent to this fluid dynamics problem. The Ms-DTM is well-installed for this purpose. - The number one advantage of Ms-DTM is its cap potential to remedy convergence troubles that may arise with the same old DTM, all without requiring restrictive simplifying assumptions. Recently, Ms-DTM has been included with Pade approximate and finite detail methods, an effective combination if you want to be critically aware of the subsequent paper.

Building upon this established foundation, the present work proposes a three-dimensional simulation of the peristaltic flow of a pseudoplastic nanofluid with variable electrical conductivity. The flow is modeled within a novel hybrid channel configuration, featuring a uniform lower wall and a non-uniform, undulating upper wall. The simulation results are presented via three-dimensional plots that illustrate the temperature and concentration distributions, velocity profiles, and streamline patterns. Quantitative validation is provided through a comparative analysis table. The structure of this paper is organized as follows: Section 2 details the mathematical formulation of the physical problem, Section 3 provides an overview of the multi-step differential transform method (Ms-DTM), and Section 4 presents and discusses the principal findings.

2 Physical Problem Structure

Hybrid channel asymmetric of Magnetohydrodynamic Pseudoplastic nanofluid is considered. The fluid moves with velocity c, and an inclined magnetic B_0

field affects the motion with inclined angel $\boldsymbol{\varepsilon}$, on Cartesian coordinates (X, Y) , see Figure 1:

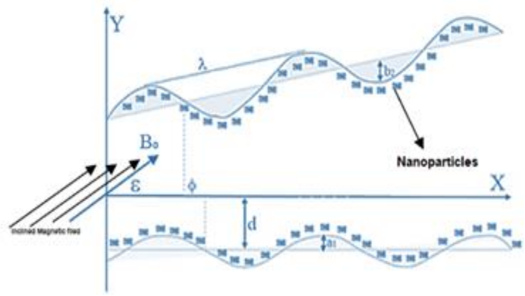

Fig. 1: fluid flow mechanism
Source: C*reated by the authors*

$$\check{d}_1(X', t') = 1 + m\,\hat{x} + b\,Sin\,\frac{2\pi}{\lambda}(x' - ct')\;Upper\;Wall \quad (1)$$

$$d_2[X', t'] = -d - a\,Cos\left[\frac{2\pi}{\lambda}\,(x' - ct') + \phi\right] \ldots.Lower\;Wall \quad (2)$$

where, the Phase $[\phi]$ difference wave $[b_2]$ amplitude for upper channel, The Lower $[d]$channel width, wave $[a]$ amplitude of Lower channel and the non-uniform $[m]$ parameter of upper channel. In addition, $0 < \phi < \pi$, wavelength $[\lambda]$. The fluid velocity can be in two-dimensional as:

$$V' = [U'(X', Y', t'), V'(X', Y', t'), 0], \quad (3)$$

As **[17],** Pseudoplastic fluid can be defined.

$$\boldsymbol{S}' = -\left\{p\left|\sqrt{\frac{1}{2}(\Delta{:}\Delta)^{n-1}}\right\}\Delta, \quad (4)$$

where, the extra stress $[S']$ tensor, the consistency $[p]$ parameter, fluid $[n]$behavior index parameter and velocity $[\Delta]$ gradient tensor the symmetric part. The fluid model generalized by many authors like [19].

Lorentz force acted the fluid flow as the following equation.

$$F' = J\times B' = \sigma(T', C')[v' \times B'] \times B' \quad (5)$$

where, $[v' = \langle U', V', 0\rangle]$ is the fluid velocity in Cartesian coordinates, $[J']$ is the current density, furthermore Dependent-electrically $[\sigma(T', C')]$ conductivity which is studied [20] and [21].

$$EC_t = EC_{25}\,[1 + \alpha(t - 25) - \beta(c - 25)] \quad (6)$$

Here, EC_t denote to the conductivity at $t\,(C^o)$, $E\,C_{25}$ denotes to conductivity at 25 (C^o), equation (6) can be dropping as the following:

$$\sigma(T', C') = \sigma_0[1 + \alpha(T' - T_0') - \beta(C' - C_0')] \quad (7)$$

Here, σ_0 is the value of electrical conductivity at constant temperature, (α) is the temperature fluid parameter, and β is the concentration fluid parameter.

The fluid model equations are stated as follows:

$$\frac{\partial U'}{\partial X'} + \frac{\partial V'}{\partial Y'} = 0, \quad (8)$$

$$\rho_f\left(\frac{\partial U'}{\partial t'}\right) = -\frac{\partial P'}{\partial X'} + \frac{\partial S'_{X'X'}}{\partial X'} + \frac{\partial S'_{X'Y'}}{\partial Y'} + \sigma(T', C')B_0^2\,\mathrm{Cos}(\varepsilon)\left(U'Cos(\varepsilon) - V'Sin(\varepsilon)\right), \quad (9)$$

$$\rho_f\left(\frac{\partial V'}{\partial t'}\right) = -\frac{\partial P'}{\partial Y'} + \frac{\partial S'_{Y'X'}}{\partial X'} + \frac{\partial S'_{Y'Y'}}{\partial Y'} + \sigma(T', C')B_0^2\,\mathrm{Sin}(\varepsilon)\left(U'Cos(\varepsilon) - V'Sin(\varepsilon)\right), \quad (10)$$

$$(\rho c)_f\frac{dT'}{dt'} = k\left[\frac{\partial^2 T'}{\partial X^{2'}} + \frac{\partial^2 T'}{\partial Y^{2'}}\right] - \frac{\partial q_r}{\partial Y'} + (\rho c)_p\left\{D_B\left(\frac{\partial C'}{\partial X'}\frac{\partial T'}{\partial X'} + \frac{\partial C'}{\partial Y'}\frac{\partial T'}{\partial Y'}\right)\right\} + \frac{D_{T'}}{T_0'}\left[\left(\frac{\partial T'}{\partial X'}\right)^2 + \left(\frac{\partial T'}{\partial Y'}\right)^2\right] - \sigma(T', C')B_0^2\left(U^{2'}Cos(\varepsilon)^2 + V^{2'}Sin(\varepsilon)^2 - 2U'V'Sin(\varepsilon)Cos(\varepsilon)\right), \quad (11)$$

$$\frac{dC'}{dt'} = D_B\left(\frac{\partial^2\bar{C}}{\partial\bar{X}^2} + \frac{\partial^2\bar{C}}{\partial\bar{Y}^2}\right) + \frac{D_T}{T_0}\left(\frac{\partial^2\bar{T}}{\partial\bar{X}^2} + \frac{\partial^2\bar{T}}{\partial\bar{Y}^2}\right) - w(T - T_0)e^{\frac{-E_a}{(\delta\theta[y]+1)}}, \quad (12)$$

where, the fluid heat $((\rho c)_f)$ capacity, the base (ρ_p) fluid density, the nanoparticle $(\rho c)_p$ heat capacity, the thermophoresis $(D_{\bar{T}})$ diffusion, the particles (ρ) density, the flow (T')temperature, (C')concentration, the (D_B)Brownian diffusion, the material and $\left(\frac{d}{dt}\right)$ time derivative,
Correspondingly, the gravity (g), coefficient (Υ) of expansion of (T), coefficient Υ^* of expansion of (C), in X', Y' separately U', V' are the velocity components.

Adapting the speeds from laboratory (X', Y') to wave (x, y) frames to obtain:

$$x' = X' - ct',\; y' = Y',\; u'(x', y') = U' - c,\; v'(x', y') = V', \quad (13)$$

After some calculations the non-dimensional parts/parameters are obtained as:
$x=\frac{x'}{\lambda}, y=\frac{y'}{d}, t=\frac{ct'}{\lambda}, h_1=\frac{h_1'}{d}, P=\frac{d^{n+1}}{c\lambda\eta_0}p, M_0=\sqrt{\frac{\sigma}{\mu}}B_0H,\ u=\frac{u'}{c}, v=\frac{v'}{c}, \delta=\frac{d}{\lambda},\ \boldsymbol{S}_{xy}=\frac{d_1\boldsymbol{S}_{xy}}{\eta_0 c}, \boldsymbol{S}_{xx}=\frac{\lambda\boldsymbol{S}_{xx}}{\eta_0 c}, \boldsymbol{S}_{yy}=\frac{\lambda\boldsymbol{S}_{yy}}{\eta_0 c}, \theta=\frac{(T'-T_0')}{(T'_1-T_0')}, Pr=\frac{\eta_0 c_p}{k}, \varphi=\frac{(C'-C_0')}{(C'_1-C_0')}, u=\frac{\partial\psi}{\partial y}, v=-\frac{\partial\psi}{\partial x},\ N_b=\frac{\tau D_B(C'-C_0')}{\nu}$

Browinian motion parameter, Thermophoresis $[N_t=\frac{\tau D_B(T'-T_0')}{\nu}]$ parameter, the stream (ψ) function, thermal (G_t) Grashoof number , and concentration (G_c) Grashoof number, thermal $\left[R_n=\frac{16}{3k^*}\frac{T_0^3}{\mu_0}\right]$ radiation, E_a is the activation energy, the electrical conductivity will take the following form.

$$\sigma(\theta,\varphi)=\sigma_0(1+\alpha\theta-\beta\varphi), \quad (14)$$

Use the above nondimensional quantites and definitions:

$$\frac{\partial p}{\partial x}=\frac{\partial}{\partial y}\left(\psi_{yy}\left[1+\xi\left(\psi_{yy}\right)^2\right]^{-1}\right)+(1+\alpha\theta-\beta\varphi)\,M^2\cos(\epsilon)^2\left(\frac{\partial\psi}{\partial y}+1\right), \quad (15)$$

$$\frac{\partial p}{\partial y}=0, \quad (16)$$

$$(1+P_rR_n)\frac{\partial^2\theta}{\partial y^2}+P_r\,N_b\left(\left(\frac{\partial\theta}{\partial y}\right)\left(\frac{\partial\varphi}{\partial y}\right)\right)+Pr\,Nt\,\left(\frac{\partial\theta}{\partial y}\right)^2+M^2Cos(\epsilon)^2\left(\frac{\partial\psi}{\partial y}+1\right)^2=0, \quad (17)$$

$$\frac{\partial^2\varphi}{\partial y^2}+\frac{N_t}{N_b}\frac{\partial^2\theta}{\partial y^2}-(\delta\theta[y]+1)\varphi[y]e^{\frac{-E_a}{(\delta\theta[y]+1)}}=0. \quad (18)$$

Eliminate pressure from the eq.(15).

$$\frac{\partial^2}{\partial y^2}\left(\psi_{yy}\left[1+\xi\left(\psi_{yy}\right)^2\right]^{-1}\right)+\frac{\partial\psi}{\partial y}\left[(1+\alpha\theta-\beta\varphi)\left[\frac{1}{D_a}\left(\frac{\partial\psi}{\partial y}+1\right)+M^2\cos(\varepsilon)^2\left(\frac{\partial\psi}{\partial y}+1\right)\right]\right]=0, \quad (19)$$

Were, Pseudoplastic nondimensional parameter [ξ]

$$S_{xy}=\left(\psi_{yy}\left[1+\xi\left(\psi_{yy}\right)^2\right]^{-1}\right), \quad (20)$$

Boundary conditions are as the follows

$$\psi=\frac{q}{2}, \frac{\partial\psi}{\partial y}=-1,\ \theta=0 \text{ and } \varphi=0 \text{ at } y=1+mx+b_2\text{Sin}[2\pi x], \quad (21)$$

$$\psi=-\frac{q}{2}, \frac{\partial\psi}{\partial y}=-1,\ \theta=1 \text{ and } \varphi=1 \text{ at } y=h_2=-d-a\,Cos[2\pi x+\phi], \quad (22)$$

3 Solution of Physical Problem

The number one intention of the usage of the multi-degree differential redesign method (Ms-DTM), applied in Wolfram Mathematica 13.2.1, is to conquer the excessive divergence regularly encountered at the same time as the use of the identical antique DTM. To follow this method, the answer interval [a, b] for the fluid version is first divided into n sub-intervals, wherein h denotes the scale of every sub-interval. The Ms-DTM is then carried out as an exceptionally correct numerical technique, facilitated with the beneficial aid of the usage of the subsequent algorithm.

$$\text{Table}[U[i]=\{\sum_{n=0}^{10}\Psi_n h^n, \sum_{n=1}^{10}n\Psi_n h^{n-1}, \frac{1}{2}\sum_{n=2}^{10}n(n-1)\Psi_n h^{n-2}, \frac{1}{6}\sum_{n=3}^{10}n(n-1)(n-2)\Psi_n h^{n-3}, \sum_{n=0}^{10}\Theta_n h^n, \sum_{n=1}^{10}n\Theta_n h^{n-1}, \sum_{n=0}^{10}\Phi_n h^n, \sum_{n=1}^{10}n\Phi_n h^{n-1}\}]. \quad (25)$$

While the multi-degree differential redesign method (Ms-DTM) has wide-ranging applications, its key benefit lies in its cap potential to treatment the divergent effects regularly encountered with the identical antique DTM. Importantly, Ms-DTM achieves this without requiring restrictive simplifying assumptions. Recently, Ms-DTM has been included with Padé approximants and finite detail methods, an effective combination to shape the primary scenario rely of the subsequent paper.

4 Results and Analytics

This has a examine proposes a singular fluid mechanics version that consists of a hybrid waft channel, thermal radiation, and chemical reactions. Using the Wiedemann-Franz regulation for metals, we deal with the fluid`s electric conductivity as a variable depending on temperature and interest. The channel geometry includes terrific parts: a non-uniform top wall and a uniform decrease wall. The evaluation relies upon into 4 subsections. The first gives a validation of the version`s accuracy via numerical comparisons, even as the closing 3-D simulations of the velocity, temperature, and interest fields, respectively.

4.1 3-D Simulation for Velocity Profile

The flow $(u(y))$ velocity behavior versus unlike values of Hartmann (M) and Pseudo parameter (ξ), temperature-dependent (α) conductivity, inclined angle (β) proposed via Figure 2, Figure 3, Figure 4 and Figure 5. It's depicted from Figure 2, Figure 3 that the fluid velocity distribution has similar effects as the Hartmann number and Pseudo parameter increases, where the velocity distribution increases at the edges of the channel and decreases at the core part of the channel. Also, opposite behavior can be found in the case of high values of the inclined parameter as shown on Figure 4.

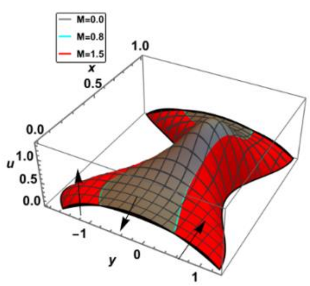

Fig 2: Velocity behavior against Harmann number (M)
Source: created by the authors

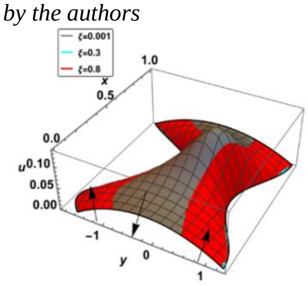

Fig. 3: velocity behavior against Pseudo parameter (ξ)
Source: created by the authors

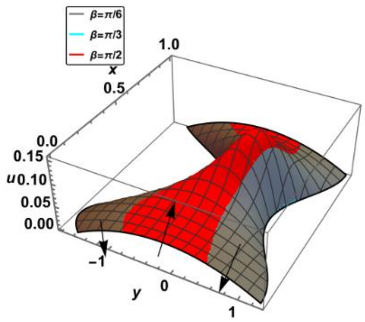

Fig. 4: velocity behavior against inclined angle (β)
Source: created by the authors

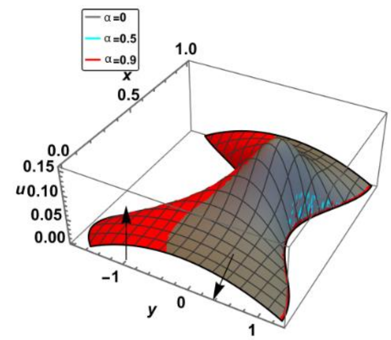

Fig. 5: velocity behavior against temperature dependent parameter (α)
Source: created by the authors

Furthermore, the temperature dependent parameter has a dual role on the fluid velocity, where the fluid velocity increases at the left-hand side of the channel and decreases at the right-hand side of the channel, as seen from Figure 5.

4.2 3-D Simulation for Temperature and Concentration Profiles

Figure 6 displays that the fluid temperature gets more energy at the right-hand side of the channel at high values of activation parameter and gets particle more energy, where it becomes freer, whilst it has an opposite behavior on the right-hand side of the channel. Also, as seen from Figure 7**,** higher values of ϵ get the fluid temperature more values, where the nanoparticle gets more freely moves. Furthermore, on Figure 8 (ρ) has an opposite behavior on the temperature of fluid. Physically, parameters like α, ρ can improve the heat transmission in solar cells

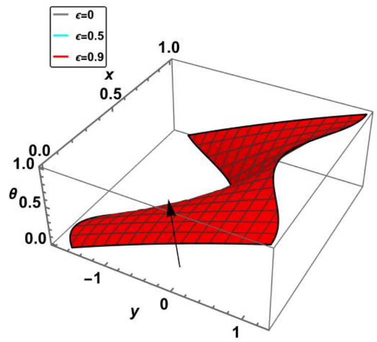

Fig. 6: Temperature behavior against Activation energy (E_a)
Source: created by the authors

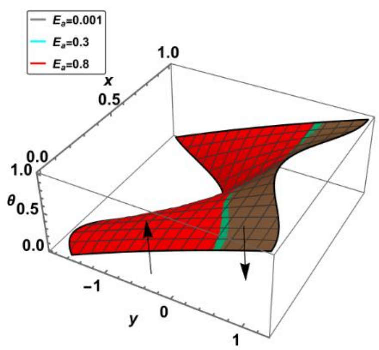

Fig. 7: Temperature behavior against (ϵ)
Source: created by the authors

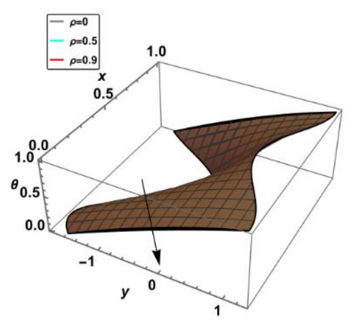

Fig. 8: Temperature behavior against (ρ)
Source: created by the authors

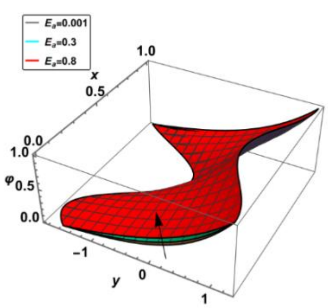

Fig. 9: Concentration behavior against (E_a)
Source: created by the authors

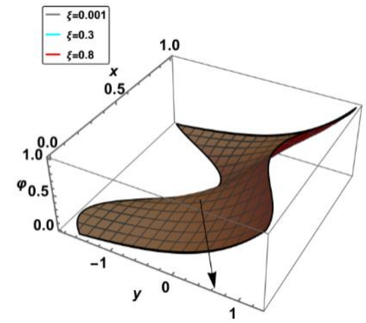

Fig. 10: Concentration behavior against N_b
Source: created by the authors

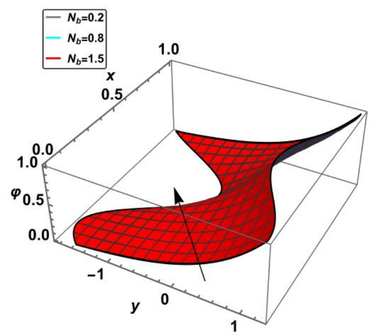

Fig. 11: Concentration behavior against ξ
Source: created by the authors

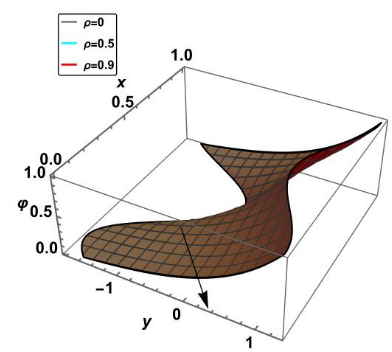

Fig. 12: concentration behavior against (ρ)
Source: created by the authors

The concentration of fluid is studied against N_b, M, E_a and ξ. It seems that the Thermophoresis parameter and Hartman number (As seen in Figure 9 and Figure 10) have an opposite relationship with pseudo parameter and the parameter of activation energy (as seen in Figure 11 and Figure 12).

Case study

Figure 13 shows a floor plan of a residential unit in a project by the New Urban Communities Authority in New October City. Model A consists of two bedrooms and a living room, with a total area of 123-129 square meters. The living room is 22 square meters, and each bedroom is 10 square meters. The exterior walls are 25 cm thick, and the interior walls are 12 cm thick. There is a 5-square-meter bathroom, a 10-square-meter kitchen, and the master bedroom has an ensuite bathroom and a terrace. It is well known that energy and its consumption are critical issues of global concern. Panic has gripped countries worldwide due to the depletion of energy resources, posing a threat to the current generation and raising concerns about the needs of future generations. Therefore, sustainability and sustainable development have emerged as a distinct approach, adopting numerous principles to conserve energy and achieve a high quality of life for all. Results show that high values of dependent-temperature and concentration electrical conductivity can get the nanoparticles more potentially energy, raising the temperature of the interior walls containing the fluid by 3-5 degrees Celsius. This results in sustainable cooling and optimal energy control. In addition, maximum velocity controls can be better using thermophoresis and Brownian motion parameters, that can improve the heat transmission in solar cells.

Fig. 13: Case Study Project
Source: created by the authors

5 Conclusions

This study presents a three-dimensional numerical simulation of the peristaltic flow of a pseudoplastic nanofluid with temperature-dependent electrical conductivity. The research investigates the potential of this system to enhance heat transfer and solar energy absorption for sustainable architectural applications. By integrating principles of fluid dynamics with building science, we propose an innovative passive cooling strategy based on circulating nanofluids within building envelopes. The proposed system is analyzed within the context of a representative residential building, modeled on projects by the New Urban Communities Authority.

Key findings include the following:

- As α increases, the walls containing the liquid gain thermal energy, as illustrated in the case study, thus we obtain optimal energy control within the insulating walls.
- E_a and ρ as a parameter of energy have an opposite behavior on the fluid concentration.
- ξ and β have a dual-contradict role on the fluid velocity.
- Without perturbation and restrictive assumptions, solutions were obtained using multi-step differential transform techniques.
- Model and solutions obtained are verified, and it seems to be good compared with the nearest published results.
- Energy saving in buildings through this application is in line with the principles of sustainable architecture and to preserve the rights of future generations to resources.
- Through this study, thermal comfort can be achieved for users of the architectural space, thus enhancing the quality of life.

References:

[1] Cooke, D. F., Goldring, A. B., Yamayoshi, I, Tsourkas P., Recanzone G. H., Tiriac, A., Pan, T., Simon, S. I., and Krubitze, L., 2012, Fabrication of an inexpensive, implantable cooling device for reversible brain deactivation in animals ranging from rodents to primates, J. Neuro. Physiol. 107: 3543–3558, 2012. DOI: 10.1152/jn.01101.2011.

[2] Hayat, T., Zahir, H., Mustafa, M., and Alsaedi, A, 2016, Peristaltic flow of Sutterby fluid in a vertical channel with radiative heat transfer and compliant walls: A numerical study, Res. in Phys., 6, 2016, 805-810. https://doi.org/10.1016/j.rinp.2016.10.015.

[3] Maria, F., Elisa, S., Enrico F. and Marco, F. Comfort Filters in a Total Energy Demand Optimization Method for the Passive Design of

a Building, Energy Procedia, 83, 2015, 418-427. https://doi.org/10.1016/j.egypro.2015.12.161.

[4] Wei J., Yang J., Gongliang L., Qing L. and Dong L., Passive nearly zero energy retrofits of rammed earth rural residential buildings based on energy efficiency and cost-effectiveness analysis, Renewable and Sustainable Energy Reviews, 180, 2023, 113300. https://doi.org/10.1016/j.rser.2023.113300.

[5] Zomorodian, Z. S., Tahsildoost, M., & Hafezi, M., 2016, Thermal comfort in educational buildings: A review article. Renewable and Sustainable Energy Reviews, 59, 895–906. https://doi.org/10.1016/j.rser.2016.01.033.

[6] Noreen, S., Kausar, T., Tripathic, D, Ain Q. U., and Lu, D., 2020, Heat transfer analysis on creeping flow Carreau fluid driven by peristaltic pumping in an inclined asymmetric channel, Ther. Sci. Eng. Prog., 17, 100486. https://doi.org/10.1016/j.tsep.2020.100486.

[7] Abdelsalam, S. I, Velasco-Hernandez, J.X., and Zaher A.Z., 2021, Electro-magnetically modulated self-propulsion of swimming sperms via cervical canal, Biomech. Mode. Mechanobiol., 20, 861–878. DOI: 10.1007/s10237-020-01407-3.

[8] Wang, H., Yao, N., Wang B., Shih, T., Wang, X., 2022, Homogeneous Venturi-effect concentrators for creeping flows: Magnifying flow velocities and heat fluxes simultaneously, Appl. Ther. Engin., 206, 118012. https://doi.org/10.1016/j.applthermaleng.2021.118012.

[9] Saleem, M., and Haider A., 2014, Heat and mass transfer on the peristaltic transport of non-Newtonian fluid with creeping flow, Inter. J. Heat. & Mass. Trans., 68, 514–526. https://doi.org/10.1016/j.ijheatmasstransfer.2013.09.053.

[10] Javid, K., Ellahi, M., Al-Khaled, K., Raza, M., Khan, S. U., Khan M. I., El-Zahar, E. R., Gouadria, S., Afzaal, M., and Khan, M. I., 2022, EMHD creeping rheology of nanofluid through a micro-channel via ciliated propulsion under porosity and thermal effects, Case Stud. Ther. Engin., 30, 101746. https://doi.org/10.1016/j.csite.2021.101746.

[11] Hasona, W., Almalki, N. H., El-Shekhipy, A. A., and Ibrahim M. G., 2020, Combined Effects of Variable Thermal Conductivity and Electrical Conductivity on Peristaltic Flow of Pseudoplastic Nanofluid in an Inclined Non-Uniform Asymmetric Channel: Applications to Solar Collectors, J. Ther. Sci. Engin. Appl., 12(2): 021018. https://doi.org/10.1115/1.4044404.

[12] Hayat, T., Iqbal, R., Tanveer, A., and Alsaedi, A., 2016, Soret and Dufour effects in MHD peristalsis of pseudoplastic nanofluid with chemical reaction, J. Mol. Liq., 220, 693–706. https://doi.org/10.1016/j.molliq.2016.04.123.

[13] Turkyilmazoglu, M., 2011, Heat and Mass Transfer on the MHD Fluid Flow Due to a Porous Rotating Disk With Hall Current and Variable Properties," J of Heat Transfer-Transactions of the ASME, 133(2): 021701. https://doi.org/10.1115/1.4002634.

[14] Ibrahim, M. G., 2022, Concentration-dependent viscosity effect on magnet nano peristaltic flow of Powell-Eyring fluid in a divergent-convergent channel, Int. Comm. Heat &Mass Trans., 134, 2022, 105987. https://doi.org/10.1016/j.icheatmasstransfer.2022.105987.

[15] Hussain, A., and Farooq, N., 2023, Gyrotactic micro-organisms swimming under the Hyperbolic Tangent Blood Nano Material and Solar biomimetic system over the Esophagus, Int. Comm. Heat &Mass Trans., 141 106579. https://doi.org/10.1016/j.icheatmasstransfer.2022.106579.

[16] Asha, S.K. and Sunitha, G., Thermal radiation and hall effects on peristaltic blood flow with double diffusion in the presence of nanoparticles, Case Studies in Thermal Engineering 17 (2020), 100560. https://doi.org/10.1016/j.csite.2019.100560.

[17] Akram S., and Afzal, Q. Effects of thermal and concentration convection and induced magnetic field on peristaltic flow of Williamson nanofluid in inclined uniform channel, European Physical Journal Plus 135 (2020) 857. DOI: 10.1140/epjp/s13360-020-00869-9

[18] Reddy, M.G., and Makindem O.D., 2016, Magnetohydro- dynamic peristaltic transport of Jeffrey nanofluid in an asymmetric channel, J. Mol. Liq. 223, 1242–1248. https://doi.org/10.1016/j.molliq.2016.09.080.

[19] Bird, R.B., Stewart, W.E., and Lightfoot, E.N., "1960", Transport Phenomena, Wiley, Singapore. DOI: 10.1002/9780470626610.

[20] Malek, J., and Rajagopal, K.R., 2005, Mathematical issues concerning the Navier–Stokes equations and some of its generalizations, in: C. Dafermos, E. Feireisl (Eds.), Evolutionary Equations, Handbook of Differential Equations, V. 2, Elsevier B.V., 1–91. DOI: 10.1016/S1874-5717(06)80008-3.

[21] Sorensen, J. A., and Glass, G. E., 1987, Ion and temperature dependence of electrical conductance for natural waters, Anal. Chem., 59, 1594−1597. DOI: 10.1021/ac00140a003.

Contribution of Individual Authors to the Creation of a Scientific Article (Ghostwriting Policy)

- M. G. Ibrahim, carried out the simulation and modeling for a mathematical model, mathematical praogramming codes, mathematical formulation section.
- Ibrahim. M. Gomaa has implemented the introduction and results sections, applications of model.
- Samar El-Sayed Ahmed was responsible for the case study of sustainable archticture, and contributed to abstract, introduction, results and discussion sections. In addition, contribute on the conclusions section and applications of mathematical model.

Sources of Funding for Research Presented in a Scientific Article or Scientific Article Itself

Self-financing.

Conflict of Interest

No conflicts of interest in this research.